Available online at www.sciencedirect.com
ScienceDirect
Trans. Nonferrous Met. Soc. China 33(2023) 3235−3249
Transactions of Nonferrous Metals Society of China
www.tnmsc.cn

# Microstructure and mechanical properties of 7075 aluminum alloy parts formed by semi-solid thixoextrusion

Guan-fei XIAO[1], Ju-fu JIANG[2], Ying WANG[3], Ying-ze LIU[2], Ying ZHANG[2], Bao-yong GUO[3], Zhen HE[1], Xi-rui XIAN[1]

1. Science and Technology on Reactor System Design Technology Laboratory, Nuclear Power Institute of China, Chengdu 610213, China;
2. School of Materials Science and Engineering, Harbin Institute of Technology, Harbin 150001, China;
3. School of Mechatronics Engineering, Harbin Institute of Technology, Harbin 150001, China

Received 7 June 2022; accepted 31 August 2022

**Abstract:** Hot-extruded 7075 aluminum alloy was used to form deep cavity cylinders by thixoextrusion. The effects of isothermal temperature and soaking time on the microstructure and mechanical properties of the formed parts were analyzed. The parameters of T6 heat treatment were optimized by orthogonal test, and the influence of T6 heat treatment on the microstructure and mechanical properties of the formed parts was studied. The results indicated that the deep cavity cylinder with a smooth surface could be successfully formed through thixoextrusion. The forming temperature and heating time had remarkable effects on the metallographic structure of the formed components. T6 heat treatment could greatly enhance the mechanical properties of the deep cavity cylinders. The optimum parameters of T6 heat treatment were achieved as: solution at 465 °C for 16 h and aging at 150 °C for 16 h. When semi-solid billets were heated at 600 °C for 10 min, the formed deep cavity cylinder had the best mechanical properties with the ultimate tensile strength of 573.57 MPa, the elongation of 13.44%, and the microhardness of HV 187.12.

**Key words:** 7075 aluminum alloy; semi-solid thixoforming; heat treatment; microstructure; mechanical properties

## 1 Introduction

7075 aluminum alloy is one of the most widely used commercial aluminum alloys in aircraft structural parts, high-strength structural parts and corrosion-resistant structural parts due to the high strength, good wear resistance and strong corrosion resistance [1−3]. At present, the manufacture of 7075 aluminum alloy parts mainly includes machining technology [4] and plastic forming methods, in which the plastic forming methods contain isothermal forging [5], hot forging [6], equal channel angular pressing (ECAP) [7], and hot-rolling [8]. Besides, due to the development of metal matrix composites, 7075 aluminum alloy composite parts have also been produced by stir casting method [9,10], and selective laser melting (SLM) [11,12]. But these processing methods are still difficult to form high performance parts with complex shapes. Hence, some effective metal forming methods need to be developed, in which the semi-solid processing (SSP) has received great attention.

Since the new metal forming method of SSP was proposed by FLEMINGS [13], it has been widely concerned. Nowadays, the theory of SSP is relatively mature, and semi-solid forming of light alloys has been widely used in automobile, 3C (computer, communication and consumer electronic)

**Corresponding author:** Ju-fu JIANG, Tel: +86-18746013176, E-mail: jiangjufu@hit.edu.cn;
Ying WANG, Tel: +86-15945697615, E-mail: wangying1002@hit.edu.cn
DOI: 10.1016/S1003-6326(23)66330-7

and other fields [14,15]. SSP technology includes rheoforming and thixoforming [13]. Cast aluminum alloys mainly adopt rheoforming for semi-solid processing [16]. Due to the advantages of semi-solid forming, many cast aluminum alloys also adopt thixoforming [17−20]. As for wrought aluminum alloy, the semi-solid temperature range with high solid fraction is wider than that of cast aluminum alloy, which is more suitable for thixoforming [21]. Recently, the development direction of thixoforming of aluminum alloys is focused on high-strength wrought aluminum alloys, and 7075 alloy is one of the most widely studied materials. Conventional thixoforming process mainly contains three steps: preparing semi-solid billets, reheating, and forming [22]. There have been many researches on the fabrication of 7075 semi-solid billets, among which strain induced melting activation (SIMA) and recrystallization and partial remelting (RAP) are the most common methods. BOLOURI et al [23] and BINESH and AGHAIE-KHAFRI [24] investigated the microstructure evolution of 7075 semi-solid billets fabricated by SIMA process. JIANG et al [25] reported the fabrication of 7075 semi-solid billets through SIMA and RAP. Besides, the thixoforming of 7075 Al alloy has also been widely studied [21,26,27]. These results indicated that the investigation of 7075 Al alloy in thixoforming was very successful. However, thixoforming has not been widely applied in industry, and one of the most important reasons is that the preparation of semi-solid billets requires long processes and high cost.

In order to broaden the application of 7075 aluminum alloy parts formed by semi-solid processing in industry, the traditional thixoforming needs further optimization to achieve a short process and low cost. XIAO et al [28] prepared 7075 semi-solid billets though a novel method named semi-solid isothermal treatment of hot-extruded aluminum alloy (SSITHEAA). In this method, the hot-extruded 7075 aluminum alloy was directly isothermal treated to obtain semi-solid billets. Compared with SIMA and RAP, this method shortens the process and decreases the cost. Besides, JIANG et al [29] successfully fabricated 5A06 aluminum alloy parts through direct semi-solid thixoforging. Therefore, the thixoforming of 7075 aluminum alloy with a short process is hopefully realized.

In this work, aiming to shorten the thixoforming process, hot-extruded 7075 aluminum alloy was used to form deep cavity cylinders by direct thixoextrusion method. Compared with the conventional extrusion, semi-solid extrusion has low deformation resistance, which is conducive to the complete filling of parts with complex shapes. At the same time, due to a certain amount of plastic deformation, the mechanical properties can also be guaranteed. Because most of the commercial raw materials of 7075 Al alloy are provided in hot-extruded or hot-rolled states, the SSITHEAA method is suitable for the fabrication of semi-solid billets before the subsequent forming. In addition, T6 heat treatment was carried out.

## 2 Experimental

### 2.1 Materials

The initial material was commercial 7075 Al alloy, which was extruded at 400 °C with the extrusion ration of 9:1. Its alloy composition (wt.%) was measured by the PW4400 X-ray fluorescence spectrometer, which was Al, 6.0 Zn, 2.3 Mg, 1.56 Cu, 0.27 Mn, 0.26 Si, 0.17 Cr and 0.03 Fe. The semi-solid temperature range was obtained from the differential scanning calorimetry (DSC) analysis, which was carried out by STA449F3 instrument with a heating rate of 10 °C/min. The results presented that the solidus temperature of this alloy was 477 °C and the liquidus temperature was 652 °C [28].

### 2.2 Thixoextrusion experiment

Figure 1 presents the two-dimensional diagram of the forming component, which was a deep cavity cylinder. The thixoextrusion process concluded the fabrication of 7075 Al semi-solid billets and the extrusion process. In this work, SSITHEAA method was utilized to fabricate semi-solid billets. The machined billets were directly placed into a box-type resistance furnace, and then heated for specified time at semi-solid temperatures. The isothermal temperatures were 580, 590, 600, 610 and 615 °C, and the soaking time was 5, 10, 15, 20 and 25 min. In this process, the original billet ($d$72 mm × 73 mm) was put into the furnace after the furnace temperature rose to the specified isothermal temperature. Because the furnace temperature would decrease in the process of placing

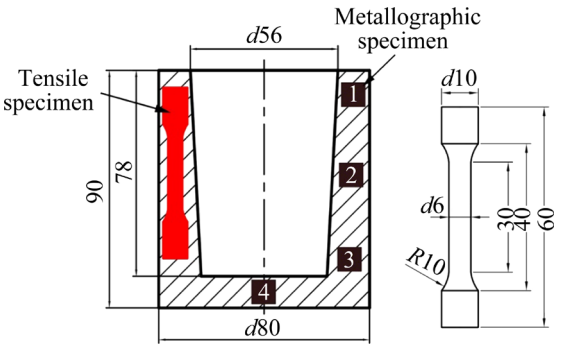


**Fig. 1** Two-dimensional diagram of deep cavity cylinder and sampling locations of metallographic specimens and tensile specimens (unit: mm)

the billet into the furnace, the soaking time was measured after the billet reached the specified semi-solid temperature. After the billet was reached the preset temperature and soaked for the specified time, it was immediately transferred from the furnace to the mold cavity (preheated to 400 °C in advance). And then, the hydraulic press started and the punch moved down. Afterwards, the loading force began to increase. As the loading force increased to the maximum (2000 kN), the maximum force was kept for 30 s, and the deep cavity cylinder was formed. In order to separate the formed part from the molds easily, the water-based graphite lubricant was used.

### 2.3 Microstructure characterization and property testing

Specimens for microstructure characterization were machined from four different locations of the formed components, and their sampling locations are shown in Fig. 1. These specimens were cut from the edge (1, 2, and 3) and the bottom center (4). The metallographic specimens were ground, polished, and then etched with Keller solution for 20−30 s. The prepared metallographic specimens were observed by an optical microscope (Olympus GX71) and a scanning electron microscope (Zeiss supra55). In addition, in order to analyze the dislocations and precipitates of the thixoformed parts, Talos F200X was used. T6 treatment was carried out on the deep cavity cylinders, and the effects of different heat treatment parameters on the mechanical properties were analyzed. The orthogonal test was carried out. Four factors were studied in this work, including solution temperature, solution time, aging temperature, and aging time, which were recorded as A, B, C, and D, respectively. Three levels were selected for each factor. The specific factors and levels are shown in Table 1. The $L_9(3^4)$ orthogonal table was selected, and the detailed heat treatment parameters are shown in Table 2. The sampling position and detailed dimensions of the tensile specimen are displayed in Fig. 1. Tensile experiments were conducted with a universal test machine (Instron 5569), and two tensile tests were carried out for each formed part. Afterwards, the fracture morphologies of the tensile specimens were observed.

**Table 1** Factors and levels of orthogonal test

| Level | A/°C | B/h | C/°C | D/h |
|---|---|---|---|---|
| 1 | 460 | 1 | 125 | 8 |
| 2 | 465 | 8.5 | 150 | 16 |
| 3 | 470 | 16 | 175 | 24 |

**Table 2** Heat treatment parameters of orthogonal test

| Number | A/°C | B/h | C/°C | D/h |
|---|---|---|---|---|
| 1 | 460 | 1 | 125 | 8 |
| 2 | 460 | 8.5 | 150 | 16 |
| 3 | 460 | 16 | 175 | 24 |
| 4 | 465 | 1 | 150 | 24 |
| 5 | 465 | 8.5 | 175 | 8 |
| 6 | 465 | 16 | 125 | 16 |
| 7 | 470 | 1 | 175 | 16 |
| 8 | 470 | 8.5 | 125 | 24 |
| 9 | 470 | 16 | 150 | 8 |

## 3 Results and discussion

### 3.1 Macro morphologies of semi-solid billet and deep cavity cylinder

Figure 2 presents the macro morphologies of the 7075 Al alloy billet and the deep cavity cylinder. Figure 2(a) shows the original cylindrical billet. Figure 2(b) shows the morphology of the billet after heating at 615 °C for 25 min, it can be found that obvious collapse occurred at the bottom of the semi-solid billet, which proved the existence of liquid phase in the microstructure. During the heating process, the billet was heated in the semi-solid temperature range, and partial liquid phase appeared. Therefore, the semi-solid billet

could not maintain the original cylindrical morphology, and the collapse phenomenon occurred at the bottom due to the effect of gravity. Figure 2(c) shows the macro morphology of the thixoformed deep cavity cylinder, in which the billet was preheated at 610 °C for 20 min before thixoforming. The formed component was completely filled and its surface was smooth. Figure 2(d) displays the macro morphology of the part (heated at 615 °C for 20 min before thixoforming) in the longitudinal section. It can be found that the surface quality of the formed part was good, the structure was compact, and there were no defects such as cracks, inclusions and shrinkages. These results indicate that the deep cavity cylinder can be formed by thixoextrusion successfully.

### 3.2 Microstructure of thixoextrusion part

As shown in Fig. 3(a), the original microstructure of the hot-extruded 7075 alloy exhibited a fibrous shape, which was composed of elongated grains and fine recrystallized grains. Figure 3(b)

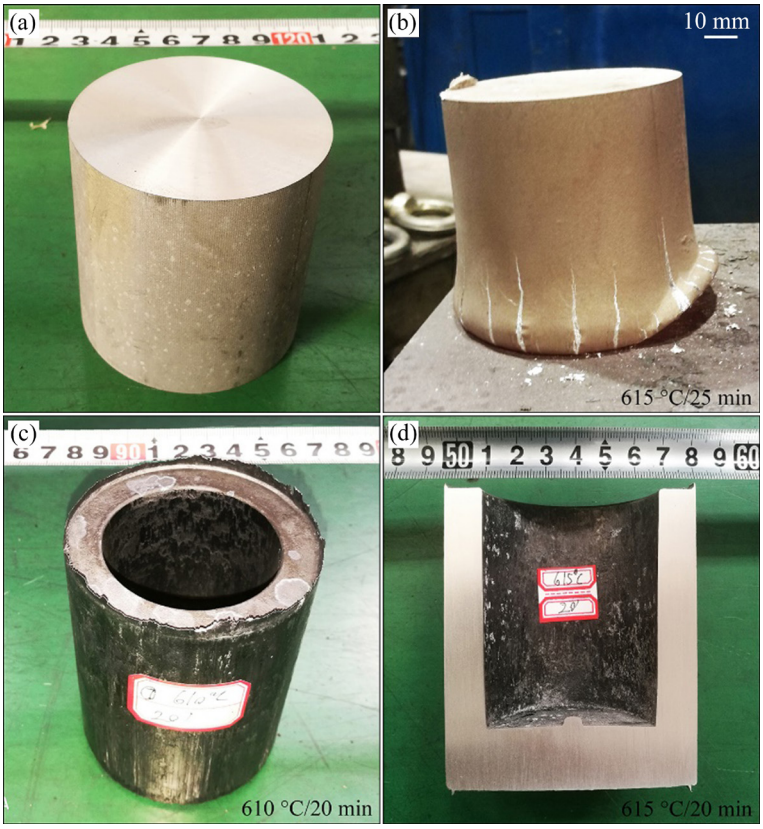


**Fig. 2** Macro morphologies of semi-solid billet and deep cavity cylinder: (a) Original cylindrical billet; (b) Semi-solid billet after isothermal treatment; (c) Thixoformed deep cavity cylinder; (d) Sectional view of deep cavity cylinder

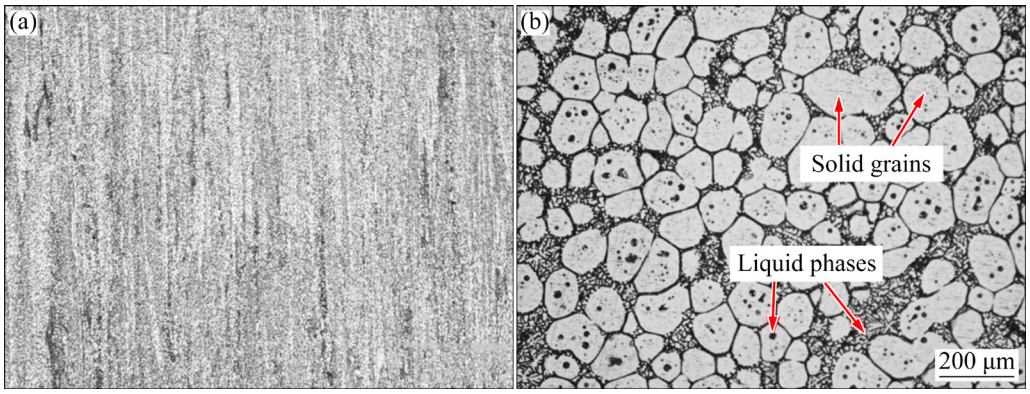


**Fig. 3** Optical microstructures of initial hot-extruded 7075 alloy (a), and semi-solid billet heated at 615 °C for 20 min (b)

presents the microstructure of the semi-solid billet heated at 615 °C for 20 min. It consisted of globular solid grains and partial liquid phases, which was beneficial to the formation of components with excellent properties. Because the hot-extruded 7075 alloy suffered large plastic deformation, enough strain energy was stored. In the subsequent isothermal treatment, the stored energy was released and the liquid phases appeared, which promoted the growth and spheroidization of solid grains. Hence, the semi-solid microstructure of 7075 alloy was obtained.

Figure 4 shows the microstructures in different locations of the deep cavity cylinder formed at 610 °C for 20 min, and the sampling locations for microstructure observation are shown in Fig. 1. The microstructure in Fig. 4(a) was composed of spherical solid grains and liquid phases (including liquid droplets and free liquid). Besides, the grain boundaries were clear and thick, which indicated that the liquid fraction of 19.4% in Location 1 was relatively high. As shown in Fig. 4(b), the microstructure in Location 2 was similar to that in Location 1, while the liquid fraction of 17.3% in Location 2 was slightly low. Meanwhile, some solid grains in Location 2 were closely connected and the coalescence phenomenon occurred (marked with red arrows) [30]. As shown in Fig. 4(c), the grains in Location 3 were squeezed together and some grain boundaries were not obvious, and the liquid fraction of 8.6% was lower than that in Location 1 and Location 2. Figure 4(d) presents the microstructure in Location 4, it can be found that there was very little liquid phase (about 2.5%) between the solid grains, and the solid grains were very small. Comparing the microstructure in different locations, it can be found that the liquid fraction decreased gradually from Locations 1 to 4. CHEN et al [27] claimed that semi-solid billet was composed of liquid phases and solid grains, and the fluidity of liquid phases was better than that of solid grains. During the forming of deep cavity cylinders, the bottom area was filled first and the top area was filled last, so the liquid phase flowed rapidly from the bottom of the deep cavity cylinders to the top during thixoextrusion. Therefore, the liquid fraction in Location 1 was the highest. However, as the liquid phase was squeezed to the upper, the solid grains remained at the bottom and suffered large plastic deformation. As a result, the proportion of liquid phase in Location 4 was very small and the solid grains were fine.

Figure 5 shows the microstructures (Location 2 in Fig. 1) of the deep cavity cylinders formed at

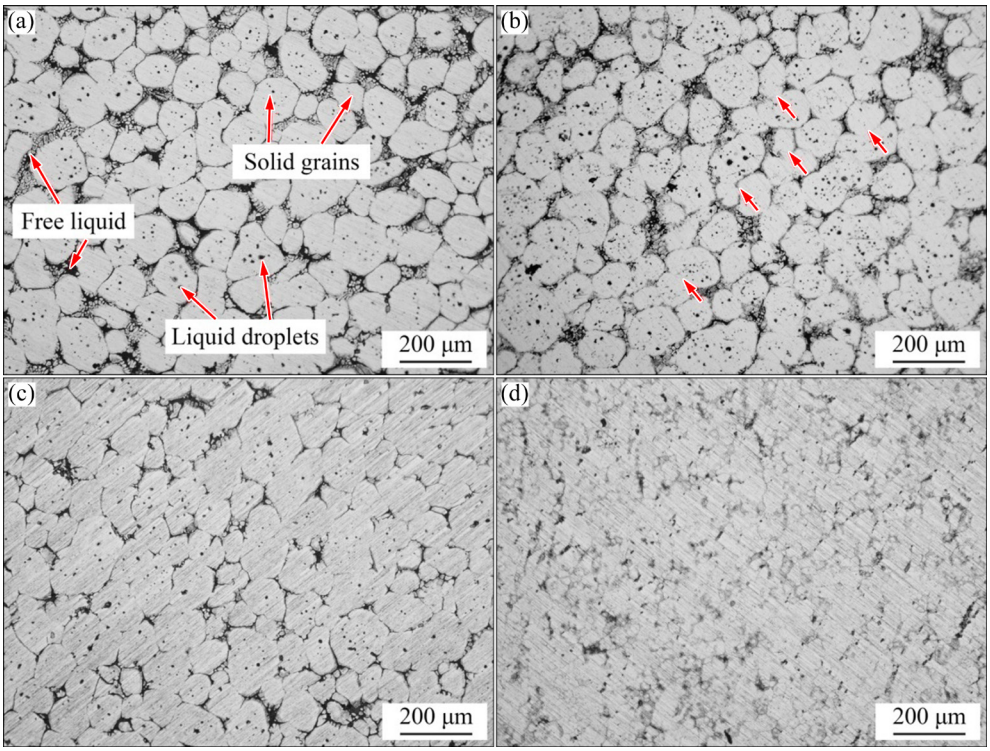


**Fig. 4** Microstructures in different locations of deep cavity cylinder formed at 610 °C for 20 min: (a) Location 1; (b) Location 2; (c) Location 3; (d) Location 4

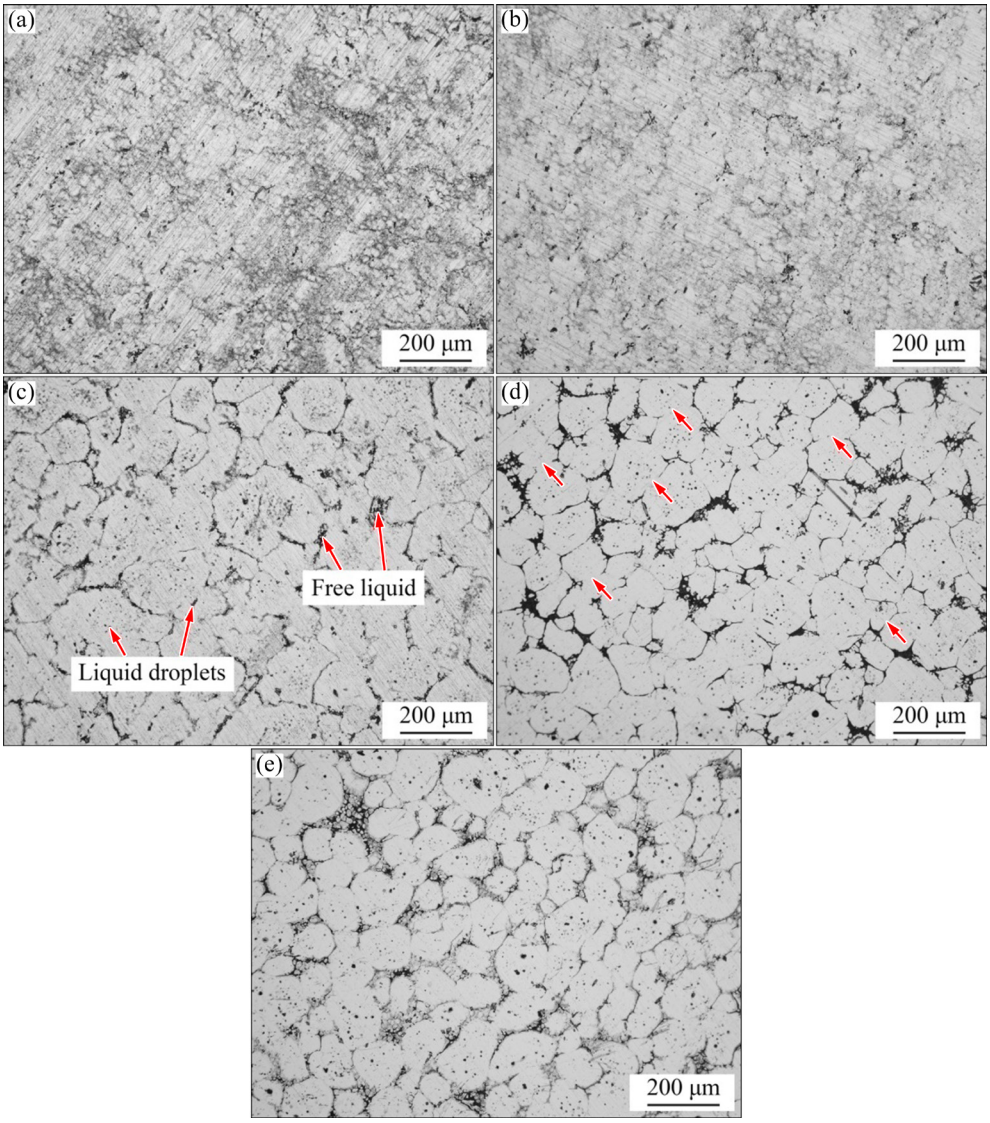


**Fig. 5** Microstructures of deep cavity cylinders formed for same soaking time of 20 min at 580 °C (a), 590 °C (b), 600 °C (c), 610 °C (d), and 615 °C (e)

various temperatures for the same soaking time of 20 min. The specific temperatures were 580, 590, 600, 610 and 615 °C, and the liquid fractions were 9.3%, 13.4%, 19.1%, 27.9%, and 34.1%, respectively. As shown in Figs. 5(a) and (b), the grains were completely squeezed together and the sizes of them were very small. At low heating temperatures (580 and 590 °C), the liquid contents in the microstructure were very low, leading to the full contact of solid grains. Hence, the deformation mechanism of solid grains was mainly dominated by the plastic deformation of solid particles (PDS) [31]. During thixoforming, these solid grains were squeezed and merged with each other, so the grain boundaries became unclear. As shown in Figs. 5(c, d, e), solid grains became rounder and the grain boundaries were relatively clear. Besides, some intragranular liquid droplets and free liquid can be observed. At high temperatures, the liquid phase proportion increased, so the fluidity of semi-solid billets was improved. Hence, the main deformation mechanisms became into the sliding between solid particles (SS) and the flow of liquid incorporates solid particles (FLS) [31]. In this process, the solid grains could flow without plastic deformation and maintain the spherical shapes. However, the liquid phases in the thixoformed part were mainly distributed in Location 1, while the liquid contents in Location 2 were slightly few. Hence, some solid grains would be close together, and the coalescence phenomenon occurred (marked with red arrows).

Figure 6 shows the microstructures (Location 2 in Fig. 1) of the deep cavity cylinders formed at 610 °C for different soaking time. At 10 min (Fig. 6(a)) and 15 min (Fig. 6(b)), the elongated solid grains with small sizes can be observed. When the soaking time was short, the liquid contents in the microstructure were very few, and the deformation mechanism was mainly the plastic deformation of solid particles (PDS). Hence, the elongated grains were observed for short soaking time. In Figs. 6(c) and (d), the solid grains became spherical and the grain boundaries were clear when the heating time increased to 20 and 25 min. Besides, the intragranular liquid droplets and the free liquid can be observed at these two soaking time. As for long soaking time, the liquid fraction in the microstructure increased, which was helpful to reduce the friction between solid grains and improve the fluidity of semi-solid billets. So, the sliding between solid particles (SS) and the flow of liquid incorporating solid particles (FLS) worked in this process, and the solid grains maintained the globular morphologies.

Figure 7 shows the SEM image and the EDS results of the deep cavity cylinder (Location 2 in Fig. 1) formed at 610 °C for 15 min. In Fig. 7(a), the eutectic phases (Point 2) and the blocky precipitates (Point 3) were distributed at the grain boundaries. The EDS results indicated that the element Al was the main alloying element in the matrix (Point 1), and the contents of other alloying elements were few inside grains. By comparison, it is easy to find that the eutectic phases (Point 2) were mainly rich in Al and Cu. Al and Cu could form low melting point precipitates, whose melting point was lower than that of the matrix, so these precipitates would melt first to form eutectic phases during isothermal treatment [32]. As shown in Fig. 7(d), Fe and Mn were rich in the blocky precipitates (Point 3). Because the precipitates with Fe and Mn obtained high melting points, they did not melt completely in the process of isothermal treatment [24]. Hence, these impurity phases with polygonal shapes were formed in the thixoextruded components.

Map scanning analysis of the deep cavity cylinder was carried out to present the distribution of alloying elements in the microstructure more visually. Figure 8 displays the map scanning results of the part (Location 2 in Fig. 1) formed at 610 °C for 20 min. It can be found that Cu was enriched at the grain boundaries. The distribution of Mg and Zn in most areas of the microstructure was relatively uniform, but the contents of them decreased slightly on the grain boundaries. The contents of Fe and Si in the initial materials were very small, so the

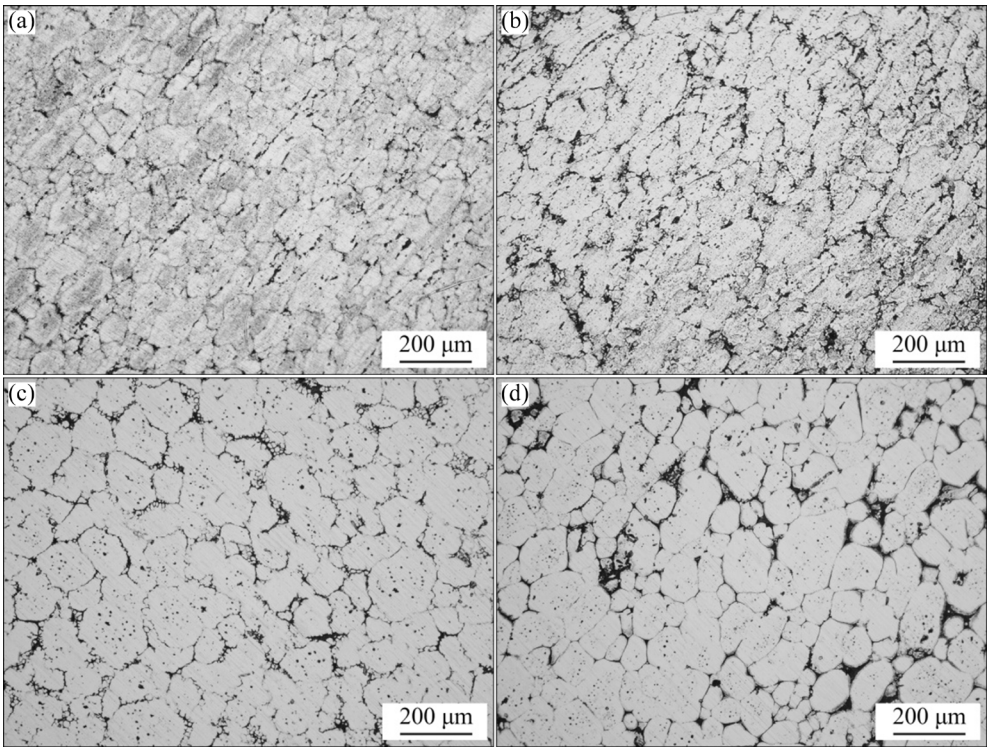


**Fig. 6** Microstructures of deep cavity cylinders formed at 610 °C for 10 min (a), 15 min (b), 20 min (c), and 25 min (d)

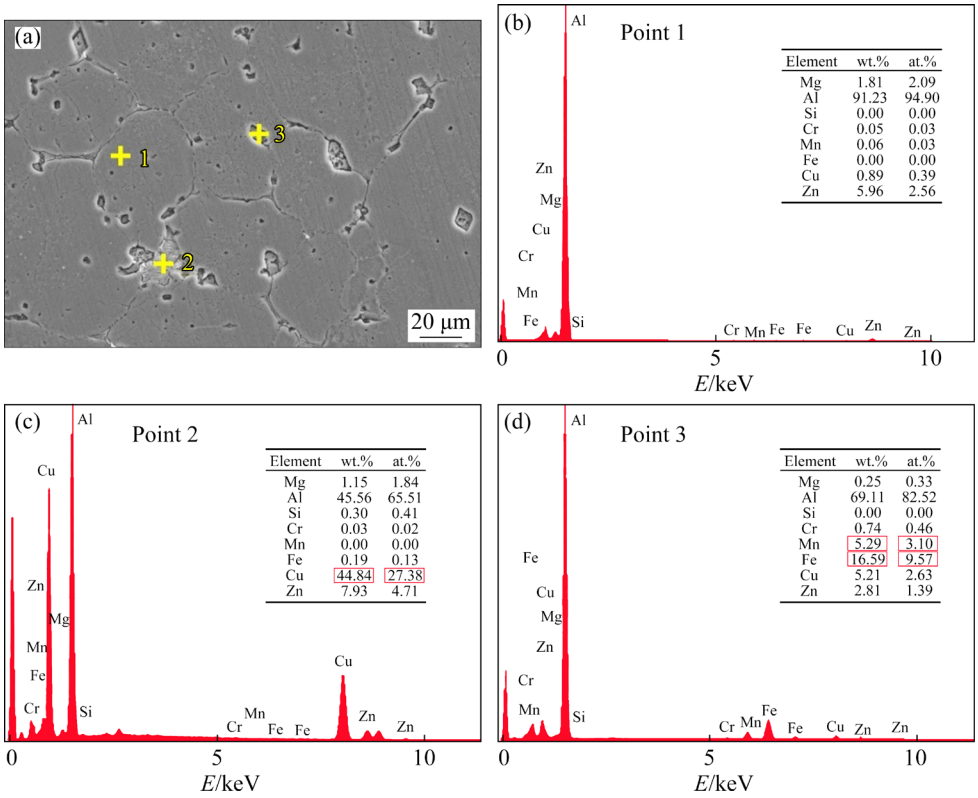


**Fig. 7** SEM image (a) and EDS results (b−d) of deep cavity cylinder formed at 610 °C for 15 min: (b) Point 1; (c) Point 2; (d) Point 3

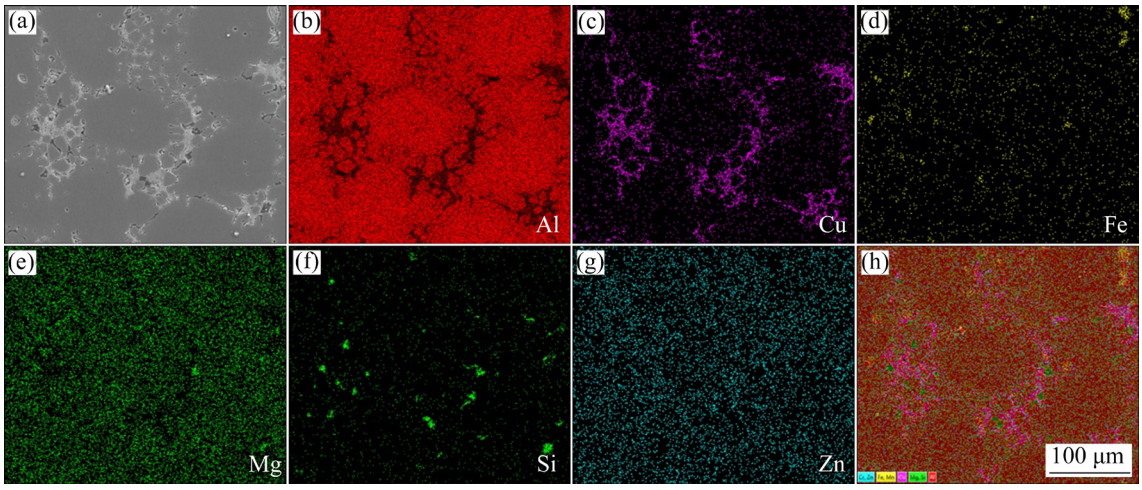


**Fig. 8** Map scanning results of part formed at 610 °C for 20 min: (a) SEM image; (b−g) Distribution of Al, Cu, Fe, Mg, Si and Zn, respectively; (h) Alloying elements

distribution of them in the microstructure of the formed parts was also limited, and they were mainly distributed at the grain boundaries.

### 3.3 Mechanical properties of deep cavity cylinder

The mechanical properties of 7075 aluminum alloy components can be greatly enhanced by T6 heat treatment [21]. In order to achieve better heat treatment effect and improve the properties of the formed parts greatly, the effects of different heat treatment parameters on the mechanical properties of the formed parts were investigated. The tensile specimens were cut from the deep cavity cylinders formed at 610 °C for 15 min. After tensile tests, the stress−strain curves in Fig. 9(a) were obtained. The obtained ultimate tensile strength (UTS), elongation (EL), and microhardness (MH) are listed in Table 3. The effects of T6 heat treatment parameters on the

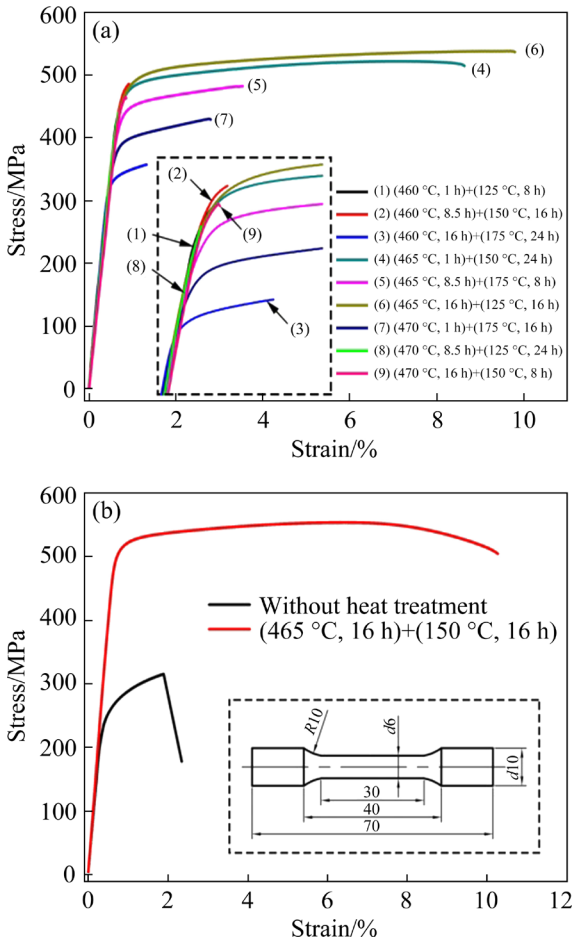


**Fig. 9** Stress−strain curves of tensile specimens: (a) After heat treatment with different parameters; (b) With and without heat treatment

**Table 3** Mechanical properties of formed parts with different heat treatment parameters

| Number | A/°C | B/h | C/°C | D/h | UTS/MPa | EL/% | MH(HV) |
|---|---|---|---|---|---|---|---|
| 1 | 460 | 1 | 125 | 8 | 460.16 | 0.78 | 170.26 |
| 2 | 460 | 8.5 | 150 | 16 | 485.59 | 0.92 | 176.00 |
| 3 | 460 | 16 | 175 | 24 | 357.14 | 1.32 | 132.46 |
| 4 | 465 | 1 | 150 | 24 | 521.95 | 9.04 | 178.22 |
| 5 | 465 | 8.5 | 175 | 8 | 482.34 | 3.53 | 165.9 |
| 6 | 465 | 16 | 125 | 16 | 538.06 | 9.80 | 187.56 |
| 7 | 470 | 1 | 175 | 16 | 429.98 | 3.12 | 154.68 |
| 8 | 470 | 8.5 | 125 | 24 | 439.78 | 0.68 | 184.42 |
| 9 | 470 | 16 | 150 | 8 | 465.33 | 2.60 | 183.66 |

mechanical properties of the formed parts were calculated by the range analysis method of orthogonal test. Table 4 presents the analysis results of the orthogonal test, in which $\bar{K}_i$ represents the mean of experiment results of level $i$, and $R$ represents the range ($R$=max($\bar{K}_i$)−min($\bar{K}_i$)). Generally, larger $R$ indicates that this factor has a greater effect on the experimental results. According to the results in Table 4, the influence order of heat treatment factors was acquired: ultimate tensile strength (UTS) A>C>D>B, elongation (EL) A>B>D>C, and microhardness (MH) C>A>D>B. Figure 10 shows the relationship between the factors and parameters. It can be found that the optimal level combination of the four factors were ultimate tensile strength (UTS) $A_2B_1C_2D_2$, elongation (EL) $A_2B_3C_2D_2$, and microhardness (MH) $A_2B_2C_1D_1$. For achieving good comprehensive properties of the deep cavity cylinders, it is necessary to consider the effects of four heat treatment factors on ultimate tensile strength, elongation, and microhardness simultaneously. According to the analysis results of the orthogonal test, the optimum level combination of the four factors was $A_2B_3C_2D_2$, and the corresponding heat treatment parameters were solution treated at 465 °C for 16 h, and aging at 150 °C for 16 h. Afterwards, the optimum heat treatment parameters were verified by experiments. Figure 9(b) displays the stress−strain curves of tensile specimens of deep cavity cylinders (formed at 610 °C for 15 min) with and without heat treatment. The ultimate tensile strength, elongation, and microhardness of the tensile specimen before heat treatment were 315.26 MPa, 1.89%, and

**Table 4** Analysis results of orthogonal test

| Parameter | Mean/ range | Factor | | | |
|---|---|---|---|---|---|
| | | A | B | C | D |
| UTS/MPa | $\bar{K}_1$ | 434.296 | 470.698 | 479.330 | 469.279 |
| | $\bar{K}_2$ | 514.119 | 469.237 | 490.956 | 484.542 |
| | $\bar{K}_3$ | 445.03 | 453.510 | 423.154 | 439.625 |
| | $R$ | 79.823 | 17.188 | 67.802 | 44.917 |
| EL/% | $\bar{K}_1$ | 1.003 | 4.312 | 3.752 | 2.302 |
| | $\bar{K}_2$ | 7.456 | 1.709 | 4.185 | 4.611 |
| | $\bar{K}_3$ | 2.134 | 4.573 | 2.657 | 3.680 |
| | $R$ | 6.456 | 2.864 | 1.528 | 2.309 |
| MH(HV) | $\bar{K}_1$ | 159.57 | 167.72 | 180.75 | 173.27 |
| | $\bar{K}_2$ | 177.23 | 175.44 | 179.29 | 172.75 |
| | $\bar{K}_3$ | 174.25 | 167.89 | 151.01 | 165.03 |
| | $R$ | 17.66 | 7.72 | 29.74 | 8.24 |

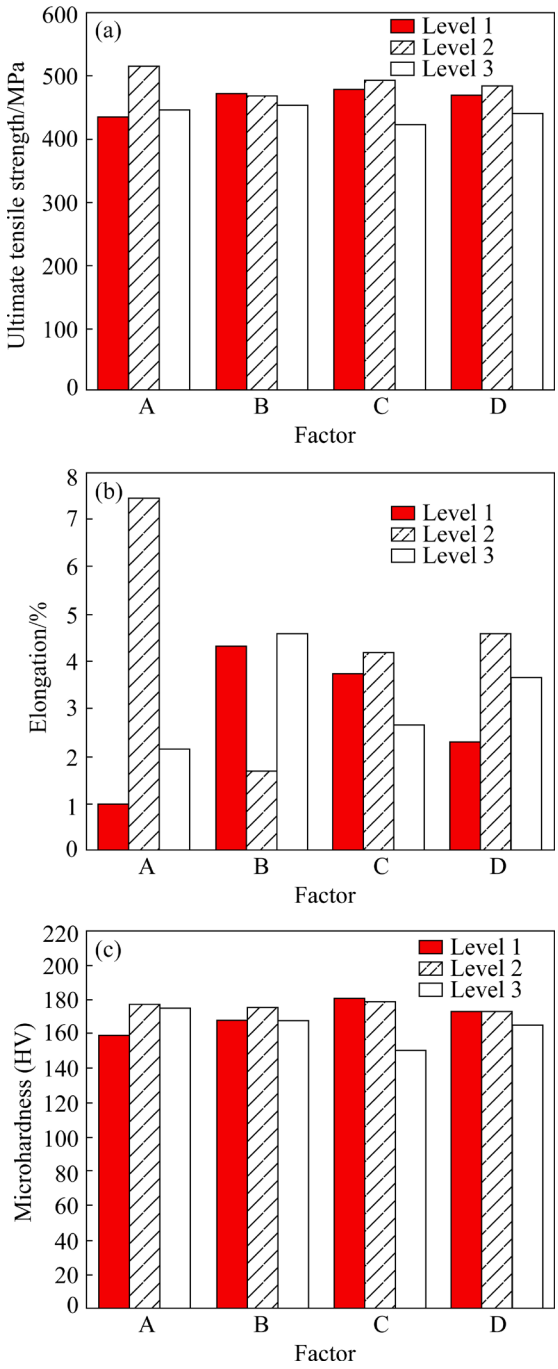


**Fig. 10** Relationship between factors and parameters: (a) Ultimate tensile strength; (b) Elongation; (c) Microhardness

HV 145.2 respectively. After heat treatment, the ultimate tensile strength, elongation, and microhardness increased to 553.15 MPa, 10.27%, and HV 184.3, respectively. The results proved that the mechanical properties of the formed components were significantly improved after heat treatment.

Figure 11 presents the effects of isothermal temperature and soaking time on the ultimate

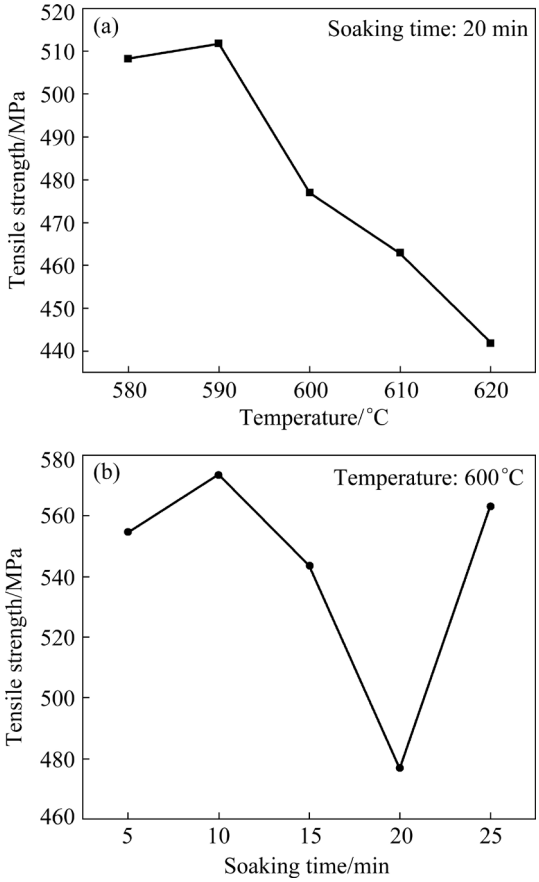


**Fig. 11** Variations of temperature (a) and soaking time (b) on tensile strength of thixoextrusion parts

tensile strength of the formed parts after T6 heat treatment. As shown in Fig. 11(a), the tensile strength increased first and then decreased with increasing isothermal temperature, and the maximum tensile strength was obtained at 590 °C. Due to the low liquid fractions at 580 and 590 °C, the solid grains in the microstructure were very small (Figs. 5(a) and (b)), and the deformation mechanism of the parts was mainly dominated by PDS. Therefore, the thixoextruded parts obtained compact microstructure and excellent mechanical properties at these two temperatures. When the heating temperature was higher than 590 °C, the mean size of solid grains increased, and the liquid fraction increased simultaneously. Hence, the plastic deformation degree of solid grains was greatly reduced and the main deformation mechanisms were SS and FLS, which resulted in the decrease of mechanical properties. Besides, the liquid segregation would occur at high temperatures because of more liquid phases. The inhomogeneous microstructure had a detrimental effect on the formed parts, leading to the reduction of tensile

strength. Figure 11(b) presents the variation of tensile strength with the soaking time. At 5 min, the recrystallization in the microstructure had just completed and there was not enough time for the solid grains to grow up. During extrusion, the plastic deformation was dominant, so the tensile strength was relatively high. At 10 min, the mean size of solid grains increased slightly, while the liquid fraction in the microstructure increased, which was helpful to improve the fluidity and filling capacity of the billets. Hence, the excellent tensile strength of 573.57 MPa was achieved at 10 min. When the soaking time was elevated to 15 and 20 min, the grain growth was obvious and the coalescence of solid grains occurred, leading to uneven grain size distribution in the microstructure. So the tensile strength decreased to 544.37 and 477.16 MPa. At 25 min, the solid grains were spherical and uniform, and many small grains were merged into large ones. The homogeneous semi-solid microstructure could reduce the liquid segregation. Hence, the tensile strength increased to 563.73 MPa. The results of all tensile tests indicated that the optimum parameters for the formation of deep cavity cylinders of the 7075 Al billets were soaked at 600 °C for 10 min. Under this condition, the ultimate tensile strength of 573.57 MPa, elongation of 13.34% and hardness of HV 187.1 were obtained.

Figure 12 shows the tensile fracture morphologies of the deep cavity cylinder formed at 600 °C for 10 min. Figures 12(a) and (b) present the fracture morphologies of tensile specimens without heat treatment, in which a few dimples can be observed, and the sizes of them were small. Besides, some micro-pits and cracks can be observed. Because the formed parts were not heat treated, some brittle phases rich in Fe and Si would appear at the grain boundaries, which would reduce the mechanical properties [21]. During tensile tests, these brittle phases were the potential crack initiation and the cracks would extend from these areas, leading to lower properties of the components without heat treatment. In Figs. 12(c) and (d), there were a lot of dimples on the fracture surface of tensile specimens after heat treatment. The large dimples were deep and well-distributed, and there were many small dimples around the larger dimples, which exhibited a ductile fracture mode [33]. During solution treatment, the precipitates at the grain boundaries would be dissolved into the matrix, and the precipitated strengthening phases would be evenly distributed in the microstructure during aging treatment. In the process of tensile

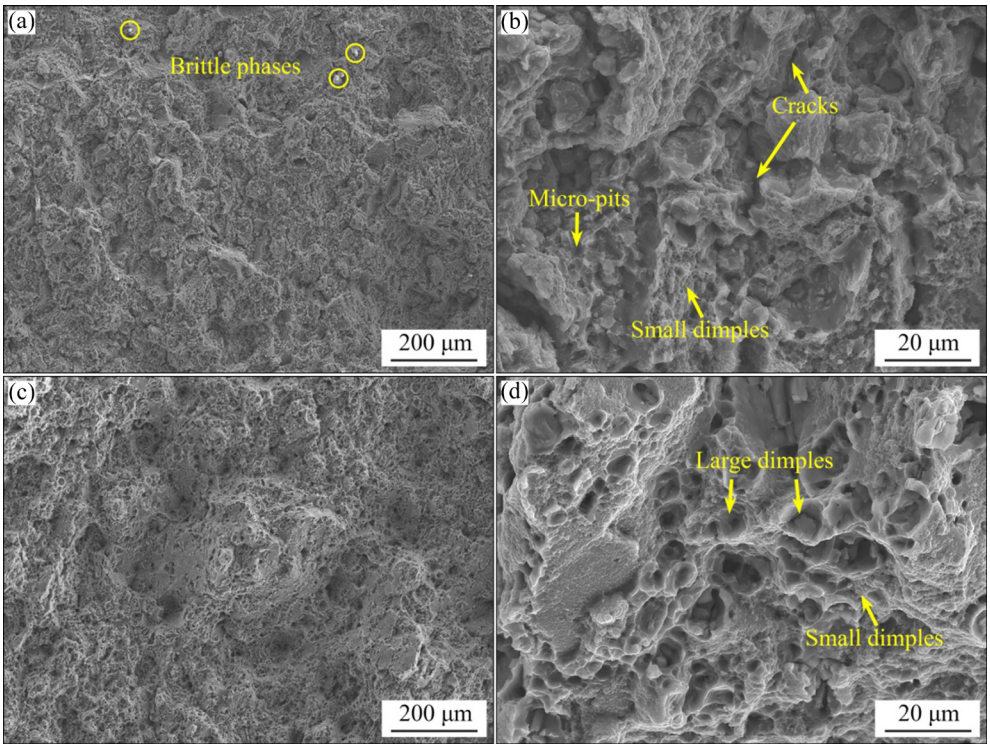


**Fig. 12** Fracture surfaces of tensile specimens of 7075 Al part formed at 600 °C for 10 min: (a, b) Without heat treatment; (c, d) With heat treatment

tests, the micro-cracks were initiated from the areas of strengthening phases, and propagated to form dimples, which led to excellent tensile strength and elongation.

Figure 13 shows the comparison of tensile properties of 7075 alloy formed through different processes. It can be found that the mechanical properties of the parts formed by thixoextrusion technology were much higher than those of the casting parts [34]. As compared with the 7075 Al parts formed by hot-rolling [8] and hot extrusion [35,36], the mechanical properties in this study were still higher. The tensile strength in this work approached to that of the wrought 7075 alloy [35] and was slightly lower than that of the parts formed by isothermal forging [37], cryorolling and room temperature rolling [38]. Compared with the traditional thixoforming [37,30,35], the mechanical properties of the components formed by direct thixoextrusion were greatly improved. It was worth noting that the elongation of the 7075 Al parts formed by direct thixoextrusion was particularly excellent. The elongation of casting parts is low due to many defects such as segregation and shrinkage porosity. Forging parts undergo a lot of plastic deformation, resulting in stress concentration, which has a certain impact on plasticity. The components formed by direct thixoextrusion have the advantages of uniform structure, no shrinkage defects, and small stress concentration, so they have high elongation. These comparisons prove that it is feasible to form high-performance 7075 Al parts by direct thixoextrusion process.

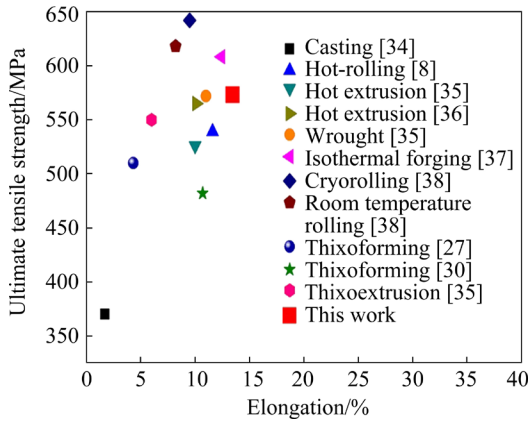


**Fig. 13** Comparison of tensile properties of 7075 Al parts formed though different processes

### 3.4 TEM analysis

Figure 14 shows the TEM images of the 7075 Al part formed at 600 °C for 10 min. Figure 14(a)

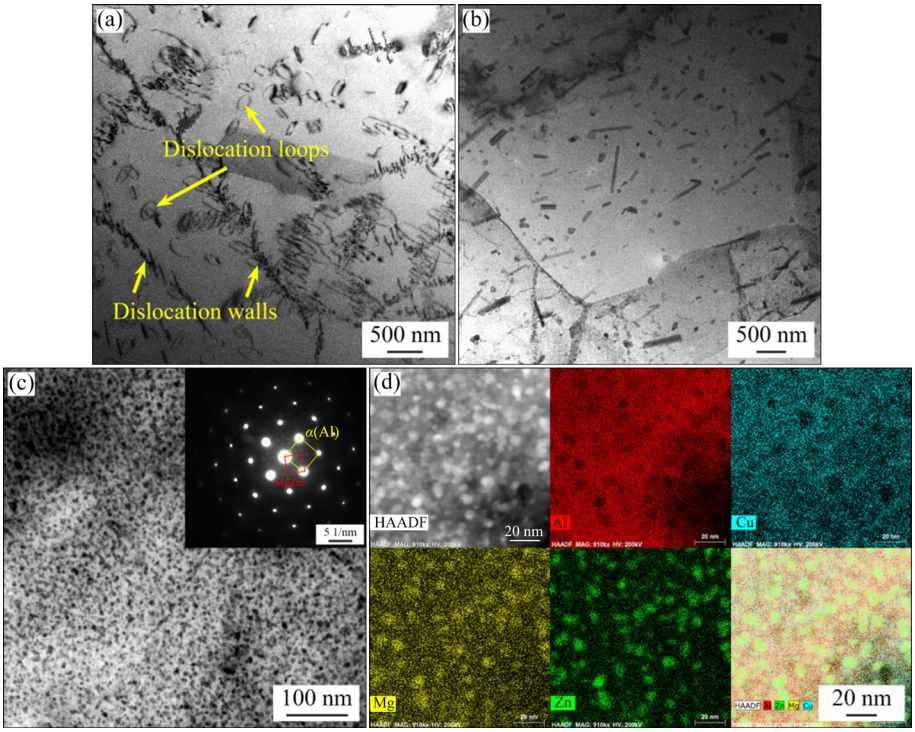


**Fig. 14** TEM images of 7075 Al part formed at 600 °C for 10 min: (a) Bright field image of specimen without heat treatment; (b) Bright field image of specimen with heat treatment; (c) Bright field image of strengthening phases; (d) EDS-mapping distribution of main elements

presents the TEM bright field image of the 7075 Al part without heat treatment, and there were some dislocations in the microstructure, including dislocation walls and dislocation loops. During thixoextrusion, the 7075 Al parts suffered some extrusion deformation, which resulted in the formation of dislocations [39]. Due to the existence of impurity phases, some dislocations would bypass the impurity particles though the Orowan dislocation bypassing mechanism, therefore, some dislocation loops were formed around the impurity particles [40]. With the increase of dislocation loops, the stress concentration was enhanced around the impurity particles, which resulted in the formation of crack source. Besides, some dislocations piled up to form the dislocation walls, which would also increase the stress concentration. Hence, the mechanical properties (UTS of 380.70 MPa and EL of 7.37%) of the formed parts without heat treatment were relatively poor. Figures 14(b, c, d) show the TEM images of the 7075 Al part after heat treatment. In Fig. 14(b), the number of dislocations was much fewer compared with that in Fig. 14(a), but the fraction of precipitates increased obviously. Because a large amount of elastic strain energy was accumulated in dislocations, some dislocations would release the elastic strain energy during heat treatment, which promoted the formation of grain boundaries and the diffusion of strengthening phases. As shown in Fig. 14(c), it can be found that the strengthening phases were well-distributed in the microstructure. Figure 14(d) presents the TEM−EDS mapping distributions of the main alloying elements. These results indicated that the strengthening phases were mainly enriched with Zn and Mg. Combined with the results of the selected area electron diffraction in Fig. 14(c) and the EDS-mapping in Fig. 14(d), it can be determined that the strengthening phase was $MgZn_2$ [41]. Due to the homogenous precipitation of strengthening phases, the mechanical properties (UTS of 573.57 MPa and EL of 13.44%) of the formed parts after heat treatment were enhanced.

## 4 Conclusions

(1) The deep cavity cylinders of 7075 Al alloy with smooth surface were successfully manufactured through direct thixoextrusion, in which the hot-extruded 7075 alloys were heated at semi-solid temperatures and then followed by semi-solid forming.

(2) The microstructures in different locations of the formed components were different. The proportion of liquid phases on the top of the formed parts was the largest, and the segregation would occur in this area.

(3) The optimum T6 heat treatment parameters of the deep cavity cylinders were investigated and optimized by orthogonal test, which were solution treated at 465 °C for 16 h and aging at 150 °C for 16 h.

(4) When the semi-solid billets were soaked at 600 °C for 10 min, the formed 7075 Al parts with T6 heat treatment obtained the best comprehensive mechanical properties with the ultimate tensile strength of 573.57 MPa, the elongation of 13.44%, and the microhardness of HV 187.12.

## Acknowledgments

This work is supported by the National Natural Science Foundation of China (No. 51875124).

## References

[1] LIU Jian, CHEN Yuan-sheng, CHAN S W N, SUNG D. Microstructure and mechanical properties of 7075 aluminum alloy during complex thixoextrusion [J]. Transactions of Nonferrous Metals Society of China, 2020, 30: 3173−3182.

[2] PANDEY V, SINGH J K, CHATTOPADHYAY K, SANTHI SRINIVAS N C, SINGH V. Influence of ultrasonic shot peening on corrosion behavior of 7075 aluminum alloy [J]. Journal of Alloys and Compounds, 2017, 723: 826−840.

[3] CHEGINI M, SHAERI M H. Effect of equal channel angular pressing on the mechanical and tribological behavior of Al−Zn−Mg−Cu alloy [J]. Materials Characterization, 2018, 140: 147−161.

[4] CAMPBELL C E, BENDERSKY L A, BOETTINGER W J, IVESTER R. Microstructural characterization of Al-7075-T651 chips and work pieces produced by high-speed machining [J]. Materials Science and Engineering A, 2006, 430: 15−26.

[5] ZHANG Yan-qiu, SHAN De-bin, XU Fu-chang. Flow lines control of disk structure with complex shape in isothermal precision forging [J]. Journal of Materials Processing Technology, 2009, 209: 745−753.

[6] JOSHI T C, PRAKASH U, DABHADE V V. Microstructural development during hot forging of Al 7075 powder [J]. Journal of Alloys and Compounds, 2015, 639: 123−130.

[7] SHAERI M H, SHAERI M, SALEHI M T, SEYYEDEIN S H, DJAVANROODI F. Microstructure and texture evolution of Al-7075 alloy processed by equal channel angular pressing [J]. Transactions of Nonferrous Metals Society of

China, 2015, 25: 1367−1375.

[8] JIANG Ju-fu, LIU Ying-ze, XIAO Guan-fei, WANG Ying, JU Ying-nan. Effect of pass reduction on microstructure, mechanical properties and texture of hot-rolled 7075 alloy [J]. Materials Characterization, 2019, 147: 324−339.

[9] KANNAN C, RAMANUJAM R. Comparative study on the mechanical and microstructural characterisation of AA 7075 nano and hybrid nanocomposites produced by stir and squeeze casting [J]. Journal of Advanced Research, 2017, 8: 309−319.

[10] SURESH S, GOWD G H, DEVA KUMAR M L S. Mechanical properties of AA 7075/$Al_2O_3$/SiC nano-metal matrix composites by stir-casting method [J]. Journal of the Institution of Engineers (India) Series D, 2019, 100: 43−53.

[11] BI Jiang, LEI Zheng-long, CHEN Yan-bin, CHEN Xi, TIAN Ze, LIANG Jing-wei, ZHANG Xin-rui, QIN Xi-kun. Microstructure and mechanical properties of a novel Sc and Zr modified 7075 aluminum alloy prepared by selective laser melting [J]. Materials Science and Engineering A, 2019, 768: 138478.

[12] OTANI Y, SASAKI S. Effects of the addition of silicon to 7075 aluminum alloy on microstructure, mechanical properties, and selective laser melting processability [J]. Materials Science and Engineering A, 2020, 777: 139079.

[13] FLEMINGS M C. Behavior of metal alloys in the semisolid state [J]. Metallurgical Transactions B, 1991, 22: 269−293.

[14] ROGAL L, KANIA A, BERENT K, JANUS K, LITYŃSKA-DOBRZYŃSKA L. Microstructure and mechanical properties of Mg−Zn−RE−Zr alloy after thixoforming [J]. Journal of Materials Research and Technology, 2019, 8: 1121−1131.

[15] JIANG Ju-fu, ZHANG Ying, WANG Ying, XIAO Guan-fei, LIU Ying-ze, ZENG Li. Microstructure and mechanical properties of thixoforged complex box-type component of 2A12 aluminum alloy [J]. Materials and Design, 2020, 193: 108859.

[16] BOLOURI A, BAE J W, KANG C G. Tensile properties and microstructural characteristics of indirect rheoformed A356 aluminum alloy [J]. Materials Science and Engineering A, 2013, 562: 1−8.

[17] DEEPAK KUMAR S, MANDAL A, CHAKRABORTY M. On the age hardening behavior of thixoformed A356−5$TiB_2$ in-situ composite [J]. Materials Science and Engineering A, 2015, 636: 254−262.

[18] DEEPAK KUMAR S, MANDAL A, CHAKRABORTY M. Effect of thixoforming on the microstructure and tensile properties of A356 alloy and A356−5$TiB_2$ in-situ composite [J]. Transactions of the Indian Institute of Metals, 2015, 68: 123−130.

[19] MATHEW J, MANDAL A, KUMAR S D, BAJPAI S, CHAKRABORTY M, WEST G D, SRIRANGAM P. Effect of semi-solid forging on microstructure and mechanical properties of in-situ cast Al−Cu−$TiB_2$ composites [J]. Journal of Alloys and Compounds, 2017, 712: 460−467.

[20] KUMAR S D, ACHARYA M, MANDAL A, CHAKRABORTY M. Coarsening kinetics of semi-solid A356−5wt.%$TiB_2$ in-situ composite [J]. Transactions of the Indian Institute of Metals, 2015, 68: 1075−1080.

[21] CHAYONG S, ATKINSON H V, KAPRANOS P. Thixoforming 7075 aluminium alloys [J]. Materials Science and Engineering A, 2005, 390: 3−12.

[22] ZHAO Cui-qing, SONG Ren-bo. Evolution of microstructure and mechanical properties for 9Cr18 stainless steel during thixoforming [J]. Materials & Design, 2014, 59: 502−508.

[23] BOLOURI A, SHAHMIRI M, CHESHMEH E N H. Microstructural evolution during semisolid state strain induced melt activation process of aluminum 7075 alloy [J]. Transactions of Nonferrous Metals Society of China, 2010, 20: 1663−1671.

[24] BINESH B, AGHAIE-KHAFRI M. Microstructure and texture characterization of 7075 Al alloy during the SIMA process [J]. Materials Characterization, 2015, 106: 390−403.

[25] JIANG Ju-fu, WANG Ying, XIAO Guan-fei, NIE Xi. Comparison of microstructural evolution of 7075 aluminum alloy fabricated by SIMA and RAP [J]. Journal of Materials Processing Technology, 2016, 238: 361−372.

[26] NEAG A, FAVIER V, BIGOT R, POP M. Microstructure and flow behaviour during backward extrusion of semi-solid 7075 aluminium alloy [J]. Journal of Materials Processing Technology, 2012, 212: 1472−1480.

[27] CHEN Gang, CHEN Qiang, QIN Jin, DU Zhi-ming. Effect of compound loading on microstructures and mechanical properties of 7075 aluminum alloy after severe thixoformation [J]. Journal of Materials Processing Technology, 2016, 229: 467−474.

[28] XIAO Guan-fei, JIANG Ju-fu, LIU Ying-ze, WANG Ying, GUO Bao-yong. Recrystallization and microstructure evolution of hot extruded 7075 aluminum alloy during semi-solid isothermal treatment [J]. Materials Characterization, 2019, 156: 109874.

[29] JIANG Ju-fu, LIU Ying-ze, XIAO Guan-fei, WANG Ying, XIAO Xin-quan. Effects of plastic deformation of solid phase on mechanical properties and microstructure of wrought 5A06 aluminum alloy in directly semisolid thixoforging [J]. Journal of Alloys and Compounds, 2020, 831: 154748.

[30] MOHAMMADI H, KETABCHI M, KALAKI A. Microstructural evolution and mechanical properties of back-extruded Al 7075 alloy in the semi-solid state [J]. International Journal of Material Forming, 2012, 5: 109−119.

[31] CHEN C P, TSAO C Y A. Semi-solid deformation of non-dendritic structures—I: Phenomenological behavior [J]. Acta Materialia, 1997, 45: 1955−1968.

[32] GEORGE S L, KNUTSEN R D. Composition segregation in semi-solid metal cast AA7075 aluminium alloy [J]. Journal of Materials Science, 2012, 47: 4716−4725.

[33] AN X L, ZHANG B, CHU C L, ZHOU L, CHU P K. Evolution of microstructures and properties of the GH4169 superalloy during short-term and high-temperature processing [J]. Materials Science and Engineering A, 2019, 744: 255−266.

[34] ZOU Xiu-liang, YAN HONG, CHEN Xiao-hui. Evolution of second phases and mechanical properties of 7075 Al alloy processed by solution heat treatment [J]. Transactions of Nonferrous Metals Society of China, 2017, 27: 2146−2155.

[35] RIKHTEGAR F, KETABCHI M. Investigation of mechanical properties of 7075 Al alloy formed by forward thixoextrusion process [J]. Materials & Design, 2010, 31:

3943−3948.
[36] ZHANG Zhi-qiang, YU Jian-hao, HE Dong-ye. Effects of contact body temperature and holding time on the microstructure and mechanical properties of 7075 aluminum alloy in contact solid solution treatment [J]. Journal of Alloys and Compounds, 2020, 823: 153919.
[37] ZHAO Jiu-hui, DENG Yun-lai, ZHANG Jin, TANG Jian-guo. Effect of forging speed on the formability, microstructure and mechanical properties of isothermal precision forged of Al−Zn−Mg−Cu alloy [J]. Materials Science and Engineering A, 2019, 767: 138366.
[38] PANIGRAHI S K, JAYAGANTHAN R. Effect of ageing on microstructure and mechanical properties of bulk, cryorolled, and room temperature rolled Al 7075 alloy [J]. Journal of Alloys and Compounds, 2011, 509: 9609−9616.
[39] FU Zhuo, WANG Zhi-feng, LI Guo-feng, YAO Yu, YU Hui, LIU Yu, ZHENG Tian-hao, XIONG Han-qing. Microstructure, mechanical and corrosion properties of Mg−1.61Al−1.76Ca alloy under different extrusion temperatures [J]. Journal of Materials Engineering and Performance, 2020, 29: 672−680.
[40] MA K K, WEN H M, HU T, TOPPING T D, ISHEIM D, SEIDMAN D N, LAVERNIA E J, SCHOENUNG J M. Mechanical behavior and strengthening mechanisms in ultrafine grain precipitation-strengthened aluminum alloy [J]. Acta Materialia, 2014, 62: 141−155.
[41] SHA G, WANG Y B, LIAO X Z, DUAN Z C, RINGER S P, LANGDON T G. Influence of equal-channel angular pressing on precipitation in an Al−Zn−Mg−Cu alloy [J]. Acta Materialia, 2009, 57: 3123−3132.

# 7075 铝合金半固态触变挤压件的显微组织和力学性能

肖冠菲[1]，姜巨福[2]，王 迎[3]，刘英泽[2]，张 颖[2]，郭保永[3]，何 震[1]，鲜希睿[1]

1. 中国核动力研究设计院 核反应堆系统设计技术重点实验室，成都 610213；
2. 哈尔滨工业大学 材料科学与工程学院，哈尔滨 150001；
3. 哈尔滨工业大学 机电工程学院，哈尔滨 150001

**摘 要**：通过触变挤压工艺对热挤压态 7075 铝合金深腔圆筒形零件进行成形，分析等温温度和保温时间对成形件显微组织和力学性能的影响。通过正交试验优化 T6 热处理工艺参数，研究 T6 热处理对成形件显微组织和力学性能的影响。结果表明，通过触变挤压可以成功成形表面光滑的深腔圆筒形零件，成形温度和加热时间对成形件的金相组织有显著影响。T6 热处理可以大大提高深腔圆筒形零件的力学性能，最优的 T6 热处理工艺参数为：465 ℃固溶 16 h，150 ℃时效 16 h。当半固态坯料在 600 ℃加热 10 min 后，成形的深腔圆筒形零件具有最佳的综合力学性能，其极限抗拉强度为 573.57 MPa，伸长率为 13.44%，显微硬度为 HV 187.12。

**关键词**：7075 铝合金；半固态触变成形；热处理；显微组织；力学性能

**(Edited by Xiang-qun LI)**